

Heterogeneous void swelling near grain boundaries in irradiated materials

S. L. Dudarev,¹ A. A. Semenov,² and C. H. Woo²

¹EURATOM/UKAEA Fusion Association, Culham Science Centre, Oxfordshire OX14 3DB, United Kingdom

²Department of Mechanical Engineering, The Hong-Kong Polytechnic University, Hung Hom, Kowloon, Hong Kong

(Received 25 July 2002; revised manuscript received 6 November 2002; published 5 March 2003)

We found that by assuming that the density of dislocations in an irradiated material varies as a function of the distance to grain boundaries and that mobile interstitial defect clusters perform *three-dimensional* diffusional motion it is possible to achieve significantly better agreement with experimental observations of profiles of heterogeneous void swelling than in the model where defects diffuse purely one-dimensionally. This approach explains the origin of several distinct features characterising the effect of heterogeneous void swelling, including the variation of the shape of swelling profiles as a function of irradiation dose, the formation of peaks of swelling and void denuded zones, and the occurrence of anomalously large voids in the regions adjacent to grain boundaries.

DOI: 10.1103/PhysRevB.67.094103

PACS number(s): 61.72.Mm, 61.80.Az, 61.82.Bg, 28.52.Fa

I. INTRODUCTION

The development of mathematical models describing materials driven far from equilibrium by irradiation¹ has recently become an important element of the international program on the development of a prototype fusion power station.² Modeling the evolution of microstructure of materials in a hostile irradiation environment³ requires investigating processes occurring simultaneously on several different time and length scales, and comparing theoretical predictions and experimental observations.

On one hand, processes occurring at grain boundaries play an important part in determining the stability of a material under irradiation. This was highlighted by recent molecular dynamics simulations of cascades occurring in a nanocrystalline metal,⁴ where it was found that the network of nanoscale grain boundaries remained stable even after crystalline order in a part of a grain was temporarily destroyed. On the other hand, by observing the evolution of microstructure in the vicinity of a grain boundary it is possible to investigate how the presence of a perturbation (in this case, a planar sink) affects the dynamics of this evolution. By studying how the microstructure of an irradiated material varies as a function of a variable introduced into the problem (here this variable is the distance to the grain boundary) one should hope to be able to understand those aspects of dynamics of microstructural evolution that cannot be addressed in the case of a spatially homogeneous system.

Spatially heterogeneous void swelling occurring in the vicinity of grain boundaries under irradiation was observed experimentally in many materials.^{5–8} Foreman *et al.*⁹ investigated whether the observed effects could be described using the so-called standard rate theory (SRT) approach proposed by Brailsford and Bullough.¹⁰ In the SRT it is assumed that single interstitial atoms and vacancies generated by irradiation in the form of Frenkel pairs diffuse three dimensionally and that the rate of absorption of interstitials by dislocations is higher than the rate of absorption of vacancies. Foreman *et al.*⁹ found that by following the SRT approach it was not possible to explain the effect of heterogeneous void swelling. Below we shall show that in fact a model *formally* similar to

the SRT, although based on different assumptions and addressing a broader range of phenomena, is able to describe experimentally observed swelling profiles in a more satisfactory way than alternative models studied in recent years.

The alternative approach, proposed by Trinkaus *et al.*¹¹ and investigated in considerable detail in Refs. 12 and 13, is based on the assumption that the effect of heterogeneous void swelling observed in the vicinity of grain boundaries is associated with purely *one-dimensional* diffusion of interstitial clusters generated by irradiation. This assumption is consistent with results of molecular dynamics simulations,^{14–17} showing that interstitial defect clusters formed in collision cascades occurring in body centered cubic (bcc) metals and in fcc metals characterized by high values of the stacking fault energy, are highly mobile. Interaction of an interstitial atom cluster with thermal phonon excitations gives rise to one-dimensional Brownian motion (diffusion) of the cluster.^{18,19} The terms “Brownian motion” and “diffusion” used in this context are equivalent. The first term refers to the motion of a single defect while the second refers to the evolution of an ensemble of defects. Detailed investigation of the model shows^{11,19} that cross-sections of reaction of mobile interstitial clusters with voids or dislocations in the material depend strongly on the dimensionality of the problem of scattering, and the predicted microstructure varies significantly depending on whether the interstitial clusters are assumed to diffuse one or three dimensionally.

The effect of heterogeneous void swelling near grain boundaries has so far been thought of²⁰ as providing a direct confirmation of the occurrence of one-dimensional diffusion of interstitial defect clusters in irradiated materials. Despite the fact that achieving quantitative agreement with experimentally observed swelling profiles proved difficult,²¹ no alternative model has been investigated so far that would stimulate carrying out more rigorous verification of concepts underlying the existing understanding of the phenomenon. The recent experimental observation⁸ of the fact that spatially heterogeneous void swelling near grain boundaries also occurs in concentrated alloys shows that at least in some cases the concept of long-range one-dimensional diffusional transport of interstitial clusters may be difficult to justify.

Indeed, the presence of compositional disorder in the crystal lattice may have a dramatic effect on the transport of interstitial defects leading to either immobilization of clusters by solute atoms through the attractive long-range elastic interactions or to the three-dimensional percolation mode of motion of clusters^{22,23} occurring in the case of repulsive elastic interaction between interstitial clusters and impurities. The tendency toward more three-dimensional diffusion of interstitial clusters in an alloy, as opposed to the purely one-dimensional diffusion occurring in a pure crystalline material, was noted in recent molecular dynamics simulations of motion of self-interstitial iron clusters in iron-copper systems.^{24,25}

The significance of interaction of mobile interstitial atoms with solute atoms and impurities follows from a simple observation that the average distance that a one-dimensionally diffusing interstitial cluster can travel in a lattice does not exceed $L = (\pi n_i r_0^2)^{-1}$, where n_i is the concentration of impurity (solute) atoms and r_0 is the effective range of elastic interaction between a mobile cluster and a solute atom. For example, in the case of a 99.99% pure material (the 0.01% concentration of helium, sodium, and magnesium impurities results from transmutation reactions in the initially 99.9999% pure aluminum irradiated by 600-MeV protons to the dose of 1 dpa⁶), where $n_i \sim 10^{19} \text{ cm}^{-3}$, we find that $L \approx 1.3 \times 10^{-5} \text{ cm}$ for the fairly modest choice $r_0 \sim 0.5 \text{ nm}$. This value of L is between one and two orders of magnitude smaller than the spatial scale (10^{-4} – 10^{-3} cm) characterizing the effect of heterogeneous void swelling near grain boundaries in irradiated materials.

This analysis has stimulated the study described below where we found that better agreement with experimental observations can be achieved by using a model that is formally very similar to the rate theory approach.^{10,26,27} The model does not require going beyond the assumption that radiation defects (this includes both single interstitials and interstitial atom clusters) perform three-dimensional diffusion. We note that this assumption *does not* contradict molecular dynamics simulations^{14–17} showing the occurrence of one-dimensional motion of defect clusters in pure materials on short time and length scales. The three-dimensional diffusion referred to in the model described below occurs on the submicron scale and results from the interaction of interstitial clusters with impurities and solute atoms giving rise to frequent random changes of the direction of the Burgers vector of diffusing clusters.^{22,23} Golubov *et al.*¹² gave a detailed analysis of features of microstructural evolution of a spatially homogeneous material that may result from constantly occurring changes in the direction of one-dimensional diffusion of interstitial clusters. The interesting aspect of our model is that, in agreement with experimental observations, we *do not* assume that the density of dislocations is a quantity independent of the distance to the grain boundary. Instead, we take it as a continuous monotonic function that vanishes at the grain boundary and reaches its asymptotic bulk value at some distance away from the boundary. The fact that “. . . few dislocations occur in the cavity denuded zone . . .” was noted by Foreman *et al.*⁹ [a similar observation was also reported in Ref. 6 where it was noted that “. . . practically no dislo-

cations (loops or line segments) were observed in the cavity denuded zone along the grain boundaries . . .”] but the conclusions drawn from the treatment developed in Ref. 9 do not agree with the solution given below.

The origin of variation of the dislocation density near grain boundaries may be either associated with elastic forces acting between a dislocation and a grain boundary²⁸ or with kinetic processes (e.g., fluctuations of the shape of dislocation lines giving rise to their attachment to grain boundaries during annealing,²⁹ or with emission and absorption of dislocations by grain boundaries^{30,31}). The occurrence of a dislocation denuded zone also correlates well with dislocation dynamics simulations showing that interacting dislocations have the tendency toward forming network structures on the micron scale.³² We note that the development of spatially heterogeneous microstructure can also occur as a result of instabilities developing in the material under irradiation.^{33,34} In our phenomenological model we do not address the dislocation dynamics aspect of the problem and instead take the profile of the density of dislocations as an arbitrary monotonic function, the shape of which may depend both on the type of the material and on the history of preparation of specimens before irradiation.

II. MODEL AND ITS SOLUTION

In this section we investigate solutions of self-consistent equations describing the evolution of concentrations of vacancies and interstitial atoms, and also the nucleation and growth of voids, in the vicinity of a grain boundary in the presence of a spatially inhomogeneous distribution of dislocations. In our model we treat vacancies and interstitial type defects (i.e., both single interstitials and self-interstitial clusters) as three-dimensionally diffusing objects. We assume that a planar grain boundary is situated at $x=0$ [i.e., that the plane of the grain boundary coincides with the (y,z) plane] and that concentrations $c_v(x,t)$ and $c_i(x,t)$ of vacancies and interstitial atoms, which are functions of distance x from the boundary, satisfy the system of two equations

$$D_\alpha \frac{d^2}{dx^2} c_\alpha(x,t) + K - \left[Z_\alpha \rho(x,t) + 4\pi \int_{t_0}^t \nu(x,\tau) a(x,t,\tau) d\tau \right] D_\alpha c_\alpha(x,t) = 0, \quad (1)$$

where index α refers to either vacancies ($\alpha=v$) or interstitial type defects ($\alpha=i$). Note that in this equation $c_i(x,t)$ does not refer to the concentration of *individual* interstitial atoms. Instead, $c_i(x,t)$ represents the effective concentration of interstitial atoms that diffuse in the lattice both individually (as single interstitial defects) and collectively (as interstitial clusters). In Eq. (1) K is the effective (inclusive of intra-cascade recombination) rate of generation of both types of defects, D_v and D_i are the effective diffusion coefficients (in the case of interstitial defects D_i is a parameter that describes both the “conventional” three-dimensional diffusion of single interstitial defects and the “forced” three-dimensional diffusion of clusters of interstitial atoms result-

ing from the interaction of clusters with solute atoms) and $\rho(x,t)$ is the density of dislocation lines. The term in square brackets describes spatial distribution of sink strengths, where $\nu(x,\tau)$ is the void nucleation rate, τ is the nucleation time and $a(x,t,\tau)$ is the radius of a void nucleated at time τ at distance x from the grain boundary. The integration over τ is performed over the interval of time between the incubation time t_0 (which is the time required to start nucleating the voids) and the moment of observation t . Z_i and Z_v are the dislocation bias factors.^{10,27} These factors describe the fact that, due to the larger formation volume of an interstitial atom defect and the resulting larger energy of its elastic interaction with a dislocation, the rate of absorption of mobile interstitials by edge dislocations is higher than the rate of absorption of vacancies. The fact that $Z_i > Z_v$ gives rise to the positive net flux of vacancies $D_v c_v - D_i c_i > 0$ to voids and leads to their nucleation and growth. Dislocation bias factors are effective parameters that enter Eqs. (1) only in the form of the product $Z_\alpha \rho(x,t)$. For convenience we normalize the value of Z_v to 1. Profiles of concentration of vacancies and interstitial defects considered as a function of time t are assumed to follow adiabatically the time dependence of the density of voids and dislocation lines. The grain boundary is treated as a perfect sink for both vacancies and interstitial atoms giving rise to the homogeneous boundary condition $c_v(0,t) = 0$ and $c_i(0,t) = 0$. We assume that the grain boundary does not migrate under irradiation, although in some cases migration may occur.³⁵ Equations (1) do not take into account the recombination of migrating vacancies and interstitial defects. This approximation is valid in the limit of low dose rates (i.e., in the limit where K is small), where the terms that are quadratic in K may be neglected.

The growth of a void situated at a distance x from the grain boundary and nucleated at time $t = \tau$ is described by the equation

$$\frac{da^2(x,t,\tau)}{dt} = 2\Theta(t-\tau)[D_v c_v(x,t) - D_i c_i(x,t)], \quad (2)$$

where $\Theta(t-\tau) = 1$ for $t > \tau$ and $\Theta(t-\tau) = 0$ for $t < \tau$. This formula is equivalent to the conventional equation describing the growth of a void due to the attachment and detachment of three-dimensionally diffusing radiation defects to the surface of the void [see, e.g., Eq. (8.29) of Ref. 27 or Eq. (5) of Ref. 13];

$$\frac{da(x,t,\tau)}{dt} = \Theta(t-\tau)[D_v c_v(x,t) - D_i c_i(x,t)]/a(x,t,\tau).$$

This latter equation is less convenient for carrying out numerical integration than Eq. (2).

In some simple cases Eqs. (1) can be solved analytically. Unfortunately, these simplified solutions do not describe actual experimental observations. We therefore need to develop a numerical procedure suitable for finding solutions of Eqs. (1) in the case where $\rho(x)$ is an arbitrary monotonic function of the distance x between a given point and the grain boundary. The requirement that the numerical procedure should retain stability in the limit of large x proves to be very significant, since in the limit $x \rightarrow \infty$ the two linearly independent

solutions of Eqs. (1) have the form $c_\alpha \sim \exp(\pm \sqrt{\rho Z_\alpha} x)$, and the presence of the exponentially growing term gives rise to instabilities similar to those known in the treatment of reflection of waves from the surface of an absorbing medium.³⁶

To solve Eqs. (1), we define a function $\Pi(x) = D_\alpha c_\alpha(x,t)$ and the spatial distribution of sink strengths $\Omega^2(x) = Z_\alpha \rho(x,t) + 4\pi \int_{t_0}^t \nu(x,\tau) a(x,t,\tau) d\tau$. Function $\Pi(x)$ satisfies the equation

$$\frac{d^2}{dx^2} \Pi(x) - \Omega^2(x) \Pi(x) = -K. \quad (3)$$

In the case $K=0$ this equation has two linearly independent solutions $\Pi_+(x)$ and $\Pi_-(x)$ satisfying asymptotic conditions $\Pi_\pm(x) \sim \exp(\mp \Omega_\infty x)$, where $\Omega_\infty = \lim_{x \rightarrow \infty} |\Omega(x)|$. Solution $\Pi_+(x)$ is regular in the limit $x \rightarrow \infty$ and $\Pi_-(x)$ diverges in this limit. The Wronskian $W(x) = \Pi_-(x) [d\Pi_+(x)/dx] - \Pi_+(x) [d\Pi_-(x)/dx]$ of these two solutions is a quantity that is independent of x for any continuous distribution of sink strengths $\Omega^2(x)$. Indeed, by differentiating $W(x)$ we find that

$$\begin{aligned} \frac{d}{dx} W(x) &= \left[\frac{d^2}{dx^2} \Pi_+(x) \right] \Pi_-(x) - \left[\frac{d^2}{dx^2} \Pi_-(x) \right] \Pi_+(x) \\ &= \Omega^2(x) \Pi_+(x) \Pi_-(x) - \Omega^2(x) \Pi_-(x) \Pi_+(x) = 0, \end{aligned}$$

and this proves that $W(x) = \text{const}$ for any continuous function $\Omega^2(x)$.

We now consider a solution of the *inhomogeneous* equation (3). Using the above property of the Wronskian, we observe that the following combination of solutions $\Pi_+(x)$ and $\Pi_-(x)$ of the *homogeneous* equation (3)

$$\begin{aligned} \tilde{\Pi}(x) &= -\frac{\Pi_-(0)}{\Pi_+(0)} \Pi_+(x) \int_0^\infty \Pi_+(x') dx' \\ &\quad + \Pi_+(x) \int_0^x \Pi_-(x') dx' + \Pi_-(x) \int_x^\infty \Pi_+(x') dx', \end{aligned} \quad (4)$$

satisfies the necessary boundary condition $\tilde{\Pi}(0) = 0$. Furthermore, by substituting this solution into Eq. (3) we find that $d^2 \tilde{\Pi}(x)/dx^2 - \Omega^2(x) \tilde{\Pi}(x) = W(x)$. Taking into account the fact that $W(x) = \text{const}$ we see that Eq. (3) can be satisfied if we choose the normalization of functions $\Pi_+(x)$ and $\Pi_-(x)$ in such a way that $W(x) = -K$.

The two solutions $\Pi_+(x)$ and $\Pi_-(x)$ of the homogeneous equation (3) required in order to construct (4) can be found by using the R-matrix algorithm,³⁶ which is described in detail in Appendix A. This completes the formal mathematical procedure that we now apply to finding profiles of concentration of interstitial atoms and vacancies in the vicinity of a grain boundary in the presence of inhomogeneously distributed dislocations.

Figures 1 and 2 show profiles of concentration calculated using the method described above for a steplike (see Fig. 1) and for an arbitrary continuous (see Fig. 2) distribution of the density of dislocations. These figures show that changes in

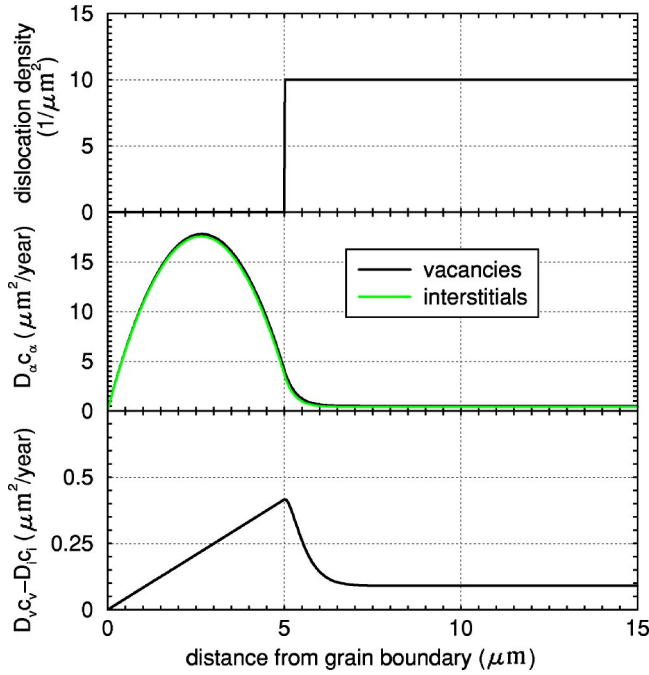


FIG. 1. Solutions of Eqs. (1) found numerically using the R -matrix method described in Appendix A for a steplike distribution of the density of dislocations $\rho(x)$. The profile of net flux of vacancies to voids $D_v c_v(x) - D_i c_i(x)$ shown in this figure is indistinguishable from that found by an analytical calculation described in Appendix B. Bias factors used in the calculation are $Z_i = 1.22$ and $Z_v = 1.0$. The relatively high value of the bias factor Z_i reflects the fact that in this model we consider the three-dimensional diffusion of interstitial clusters that interact with dislocations stronger than single interstitial atoms (Ref. 12). The dose rate K equals 5 dpa/year.

the shape of the profile of the density of dislocations $\rho(x)$ affect the profiles of concentration of mobile vacancies and interstitial defects. In the case of a step-like profile $\rho(x)$ shown in Fig. 1 the net flux of vacancies to voids varies linearly as a function of x in the dislocation-free zone. This agrees with the analytical solution of the problem given in Appendix B. On the other hand, in the case where $\rho(x)$ is a smooth monotonic function of variable x (see Fig. 2), the shape of the net vacancy flux profile depends on the distribution of the density of dislocations in a more complex way, which is difficult to describe using analytical approximations.

Further study of kinetics of inhomogeneous swelling requires introducing a model describing the nucleation and growth of voids. Experimental data discussed in previous publications^{9,13,21} refer to the interval of relatively low irradiation doses where voids continue to nucleate over the entire period of observations. The experimental data described in Ref. 9 show that the visible volume concentration of voids increases approximately linearly with the irradiation dose. This suggests that in this interval of irradiation doses nucleation is almost unaffected by the presence of existing voids. Moreover, since the observed nucleation rate remains relatively high over the interval of doses studied experimentally, we can assume that thermal emission of vacancies from

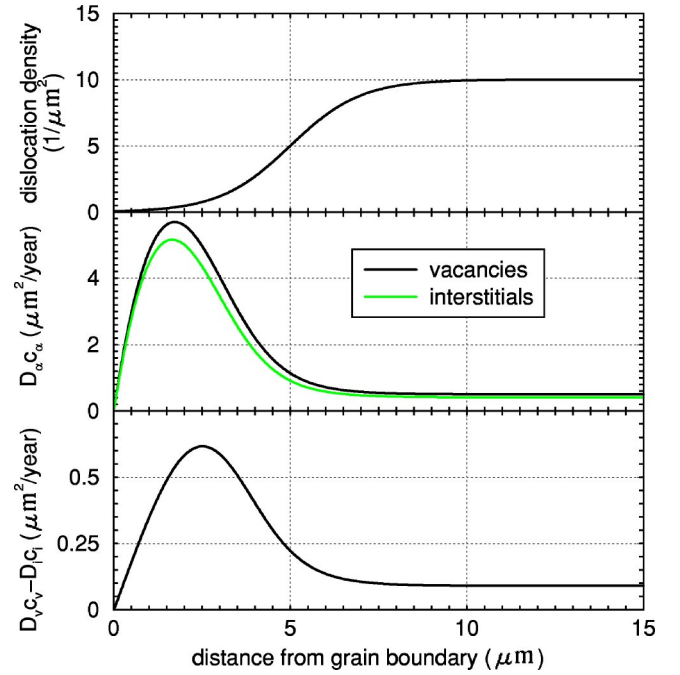


FIG. 2. Solutions of Eqs. (1) found numerically using the R -matrix method described in Appendix A for a smooth but otherwise arbitrarily chosen distribution of the density of dislocations $\rho(x)$. The asymptotic bulk value of the density of dislocation lines, the bias factors and the dose rate remain the same as those shown in Fig. 1. Note that the maximum value of function $D_v c_v - D_i c_i$ shown in this figure is greater than the maximum value of the same function calculated for a step-like distribution of the density of dislocations shown in Fig. 1.

voids does not significantly influence the nucleation process or, in other words, the critical radius of voids remains small. In this case we may treat the process of nucleation of voids as diffusion of the population of voids in the *size* space, where nucleation and growth is driven by the net flux of vacancies to voids $D_v c_v - D_i c_i$ competing against random fluctuations of fluxes of vacancies and interstitials. Taking into account the fact that the amplitude of fluctuations of fluxes of point defects is proportional to $D_v c_v + D_i c_i$ (see Ref. 37 for more details), we find that the rate of nucleation of voids is given by³⁸

$$\nu(x,t) = \mathcal{R}K \frac{D_v c_v(x,t) - D_i c_i(x,t)}{D_v c_v(x,t) + D_i c_i(x,t)}, \quad t > t_0, \quad (5)$$

where \mathcal{R} is a rate factor that remains constant over the interval of irradiation doses studied experimentally. We now investigate self-consistent solutions of Eqs. (1), (2), (4), and (5), and study the evolution of the spatially inhomogeneous distribution of voids nucleating and growing in the vicinity of a grain boundary.

III. RESULTS AND DISCUSSION

We start by summarising the experimental findings. There are several significant features characterising the phenomenon of heterogeneous void swelling that a suitable theoret-

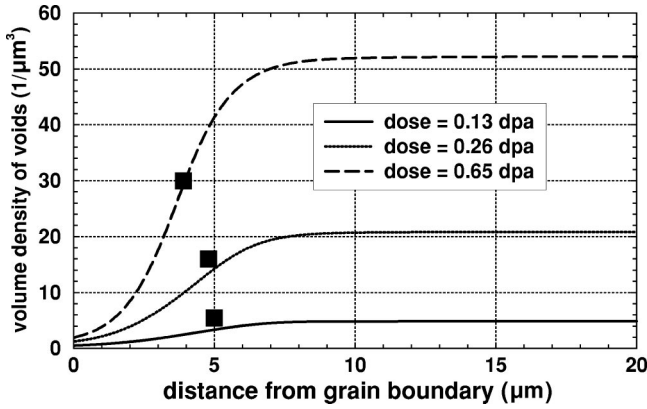


FIG. 3. Density of voids evaluated self-consistently using Eqs. (1), (4), and (5) for $\mathcal{R} = 10^3 \text{ micron}^{-3} \text{ dpa}^{-1}$. Profiles shown in this figure were calculated for the three values of the irradiation dose corresponding to experimental data given by Foreman *et al.* in Ref. 9. The density of voids drops by more than an order of magnitude in the region adjacent to the grain boundary resulting in the formation of a void denuded zone. Dislocation bias parameters used in the calculations are $Z_i = 1.22$ and $Z_v = 1.0$. Boxes represent void densities measured experimentally.

ical model should be able to address. They are (i) the relatively large spatial scale of void swelling profiles, (ii) the occurrence of void denuded zones in the regions adjacent to grain boundaries (see for example Fig. 3 of Ref. 6), (iii) the nearly symmetric shape of void swelling peaks (this point is particularly difficult to address using the existing models²¹), and (iv) the origin of rare but unusually large voids often observed near grain boundaries in the void denuded zones (these large voids can be clearly seen in Fig. 3 of Ref. 5, and in Fig. 3 of Ref. 6). We should also note that in some cases peaks of void swelling were not observed at all³⁹ and the spatial scale characterizing the effect was fairly small.

We begin by arguing that the assumption that the density of dislocation lines can be approximated by a function independent of the distance to the grain boundary (this approximation was adopted in a recent study⁴⁰) does not represent the best possible starting point for the treatment of the problem. Indeed, the presence of image forces acting between a grain boundary and a dislocation (see Ref. 28 for a comprehensive review of the subject) should inevitably lead to the formation of zones *denuded of dislocations* (not voids yet) in the vicinity of grain boundaries in well annealed materials. This conclusion does not depend on whether the interaction is attractive or repulsive, since in the first case the dislocations will be absorbed by the grain boundary while in the second case they will be pushed away from the boundary in the interior region of the grain. Note also that the weakness of elastic forces acting between a dislocation and a grain boundary is compensated for by the very long time available during the annealing process for the development of the microstructure (the experimental data described in Ref. 9 were obtained using well annealed samples, and the authors of Refs. 9 and 6 confirmed that only few dislocations were observed in the cavity denuded zone). Fluctuations of the shape of dislocation lines at high temperatures should also lead to the formation of zones free from dislocations as a result of

attachment of dislocations to grain boundaries.²⁹ It is therefore natural to treat the problem of void swelling starting from a monotonic profile of the density of dislocations $\rho(x)$, where function $\rho(x)$ vanishes at $x=0$ and where $\rho(x)$ reaches its asymptotic bulk value at a certain distance away from the grain boundary. It is also reasonable to assume that the overall density of dislocation lines should increase under irradiation as a result of growth of dislocation loops. Also, it is likely that the climb of dislocations should give rise to dislocations propagating from the interior region of the grain towards grain boundaries during irradiation.

Following these arguments, we approximate the density of dislocation lines by a simple analytical formula (in qualitative terms the results reported below are not sensitive to the particular choice of the shape of this profile)

$$\rho(x,t) = \rho_0(t) \frac{\exp(-w/x)}{1 + \exp[-(x-x_0(t))/w]}, \quad (6)$$

where $\rho_0(t)$ and $x_0(t)$ are assumed to vary slowly as a function of irradiation time. The function given by Eq. (6) vanishes in the limit $x \rightarrow 0$ and reaches its bulk asymptotic value $\rho(x) \rightarrow \rho_0(t)$ in the limit $x \rightarrow \infty$. The irradiation time t is related to the dose ϕ via $\phi = Kt$.

Figure 3 shows the distribution of the volume density of voids calculated for the three values of irradiation dose for which experimentally observed values were reported in Ref. 9. The incubation dose ϕ_0 corresponding to the onset of void growth t_0 is assumed to be equal to 0.08 dpa. Values of the density of voids at swelling peaks observed experimentally were $N_v^{(\phi=0.13\text{dpa})} = 5.5 \text{ micron}^{-3}$, $N_v^{(\phi=0.26\text{dpa})} = 16 \text{ micron}^{-3}$, and $N_v^{(\phi=0.65\text{dpa})} = 30 \text{ micron}^{-3}$. These values agree reasonably well with the calculated values $N_v^{(\phi=0.13\text{dpa})} = 3 \text{ micron}^{-3}$, $N_v^{(\phi=0.26\text{dpa})} = 10 \text{ micron}^{-3}$, and $N_v^{(\phi=0.65\text{dpa})} = 28 \text{ micron}^{-3}$, representing void densities at distances corresponding to peaks of void swelling profiles discussed below.

Profiles of the density of dislocations [Eq. (6)] are assumed to evolve with irradiation dose as shown in Fig. 4. Given the overall functional form of the dislocation density profile [Eq. (6)], the parameters x_0 , w and the rate of increase of the asymptotic bulk density of dislocations $\rho_0(t)$ have been chosen to reproduce the experimentally observed profiles of void swelling shown in Fig. 5. Other choices of input parameters of the model give rise to profiles qualitatively similar to those shown in Fig. 5. Here, void swelling was calculated by using Eqs. (2) and (5), where the concentrations c_v and c_i were evaluated self-consistently via Eqs. (1). The comparison of calculated and observed profiles shows that by using the present model it is possible to achieve good agreement with experiment both in terms of the shape of the profiles and also in terms of the calculated and observed values of void swelling in the interior region of the grain. None of this was possible within the framework of models considered previously.^{11,21}

Note that profiles shown in Fig. 4 and representing the variation of the density of dislocations as a function of the distance to the grain boundary agree reasonably well with experimental measurements (The authors are grateful to Pro-

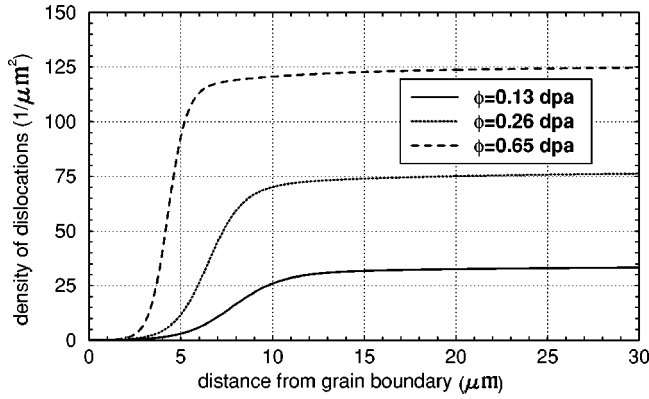


FIG. 4. Snapshots of profiles of the density of dislocation lines used in the study of solutions of Eqs. (1). The profiles are described by analytical expression (6), where the width of the transition region w , the distance between the centre of the transition region x_0 and the grain boundary, and the asymptotic bulk value of the dislocation density ρ_0 were assumed to vary slowly as a function of the irradiation dose. Note that the density of dislocations shown in this figure represents an effective parameter consistent with the choice of normalization of the bias factor $Z_v = 1$. Other possible choice of values of bias factors will require simple re-scaling of curves shown in this figure.

fessor M. Victoria for giving us access to these experimental data) reported in Ref. 41. In the case of aluminum irradiated to the dose of 1.1 dpa by 590 MeV protons at $T = 390$ K the observed density of dislocations was found to be $\rho_0 = 7.0 \times 10^{13} \text{ m}^{-2}$, which is equal to $\rho_0 = 70 \text{ micron}^{-2}$. This value compares very well with the value of $\rho_0(t) = 125 \text{ micron}^{-2}$ corresponding to $\phi = 0.65$ dpa found using our model. Indeed, at higher doses the density of dislocations does not increase as rapidly as it does in the limit of small doses [the calculated value of $\rho_0(t)$ at $\phi_0 = 1$ dpa is 140 micron^{-2}]. Moreover, we should emphasize that the density of dislocations enters Eqs. (1) only in the form of the product ρZ ,

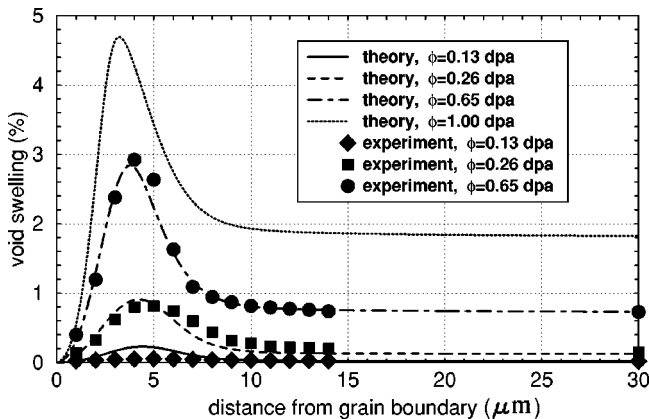


FIG. 5. Profiles of void swelling calculated numerically using self-consistent equations (1)–(5) for the three values of the total irradiation dose where experimental data are available (Ref. 9), and also for a somewhat larger value of the dose illustrating the absence of the immediate saturation of void swelling exhibited by the model. Bias factors used in the calculations are $Z_i = 1.22$ and $Z_v = 1.0$.

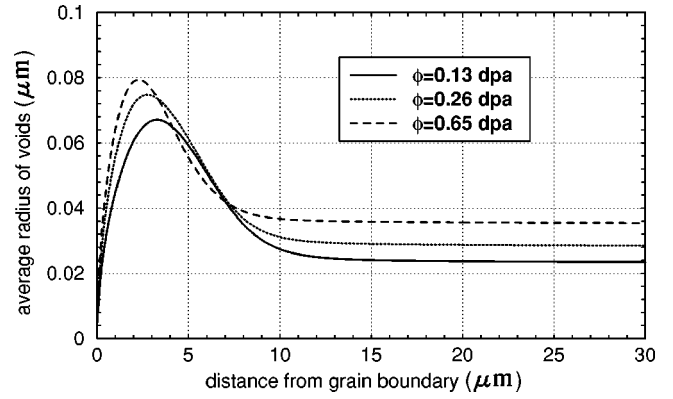


FIG. 6. Profiles illustrating the evolution of the average radius of growing voids considered as a function of the distance to the grain boundary. The average radius of the void \bar{a} is defined as $\bar{a} = (3S_v/4\pi N_v)^{1/3}$, where S_v represents the local void swelling and N_v is the local volume density of voids. By comparing results shown in this figure with those shown in Fig. 3 we find that the density of voids in the region immediately adjacent to the grain boundary is substantially lower than that in the interior of the grain. At the same time the average size of voids growing near the boundary exceeds significantly the average size of voids growing in the interior region of the grain.

where Z is the bias factor. In our treatment we choose to normalize the vacancy bias factor to unity $Z_v = 1.0$. In practice the values of bias factors Z may vary in the range between 1 and 5 (Ref. 27) (indeed, it is not the absolute value of Z_i or Z_v but the ratio Z_i/Z_v that plays the main part in determining the rate of void swelling) and the choice of normalization $Z_i = 2.44$ and $Z_v = 2.0$ would bring the values of $\rho_0(t)$ used in our model calculation into exact agreement with experimental measurements.

A particularly important feature characterizing the effect of inhomogeneous void swelling is the occurrence of unusually large voids in the void denuded zones adjacent to grain boundaries. The rarely distributed large voids situated very close to grain boundaries can clearly be seen in electron microscope images given in Refs. 5 and 6. None of the models investigated so far was able to explain the very striking observation that the rate of *growth* of voids can be higher in the regions where the *nucleation* of voids is suppressed. Figure 6 shows how this phenomenon can be understood using Eqs. (1). The average radius \bar{a} of a void is a quantity related the local value of void swelling S_v and the local density of voids N_v via

$$S_v = \frac{4}{3} \pi N_v \bar{a}^3.$$

A comparison of profiles shown in Figs. 3 and 5 shows that a substantial part of each swelling peak is situated in the region where the density of voids is low. The fact that values of local swelling remain high in the region where the density of voids is low shows that the average size of voids in this region can be substantially greater than the size of voids growing in the interior of the grain. The occurrence of large voids in the vicinity of grain boundaries is associated

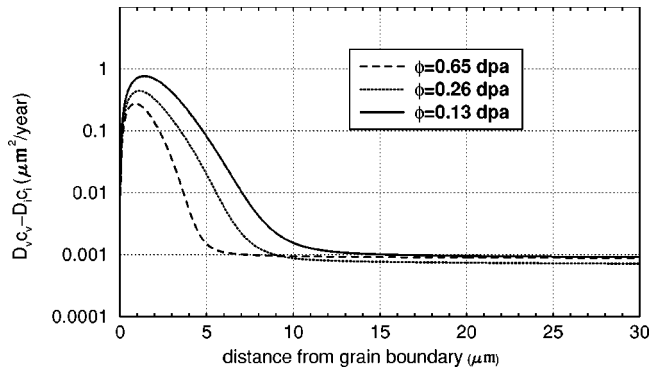


FIG. 7. This figure shows how the net vacancy flux to voids $D_v c_v - D_i c_i$ varies as a function of distance x to the grain boundary and as a function of irradiation dose. The peak of function $D_v c_v(x) - D_i c_i(x)$ in the vicinity of the grain boundary is associated with low total density of sinks in that region. The gradual drift of the peak of the void size profile towards the grain boundary visible in Fig. 6 is related to the evolution of the profile of the net vacancy flux shown in this figure.

with the low density of sinks in the regions adjacent to the boundaries and the resulting high local values of the net vacancy flux $D_v c_v - D_i c_i$. Figure 7 illustrates this point in more detail.

The model considered above makes it possible to comment on cases where the effect of inhomogeneous void swelling near grain boundaries was *not* observed, see, e.g., the case of void swelling under electron irradiation described in Ref. 39. On the one hand, in the model where we assume that interstitial defects perform three-dimensional diffusion, the presence of a *dislocation* denuded zones near grain boundaries prior to irradiation is necessary to explain the formation of the peak of void swelling situated at a certain distance from the grain boundary. In the case where the distribution of the density of dislocations is homogeneous across the grain, no peak of void swelling are expected to occur, and this may explain their absence in experiments described in Ref. 39. There are other even more fundamental reasons that can be responsible for the difference between experimental observations corresponding to cases of electron and neutron/ion (cascade) irradiation. It is often assumed that the main difference between the two cases is associated with the fact that electron irradiation produces Frenkel pairs of defects while cascade irradiation generates clusters of defects, and the difference between scenarios of microstructural evolution occurring in the two cases is associated with the occurrence of one-dimensional diffusion of interstitial clusters. A more thorough examination shows that there are other significant differences, namely, (i) the presence of transmutation reactions in the case of neutron irradiation giving rise to the accumulation of helium *and* other impurities in the material,⁴² (ii) the presence of new mechanisms of nucleation associated with the direct formation of nanovoids in cascades as opposed to nucleation occurring via the sequential accumulation of vacancies in vacancy clusters, and (iii) the difference in the magnitude of the dislocation bias factors (the effective value of the ratio Z_i/Z_v describing the interaction of mobile interstitial clusters with dislocations may be

significantly higher than that characterizing the case of single interstitial atoms¹²). Furthermore, (iv) we should expect that in the case of electron irradiation the high concentration of single interstitial atoms will give rise to the rapid climb of dislocations. In the case of neutron irradiation pinning by interstitial clusters investigated in Refs. 43,44 impedes the motion of dislocations, and the resulting evolution of the dislocation component of the microstructure, as well as void swelling profiles, should be expected to differ significantly from the case where pinning of dislocations by interstitial clusters does not occur.

Results described above show that the conclusion drawn in Ref. 9 regarding the point that a rate theory-type approach assuming the dominance of three-dimensional diffusion of defects could not describe heterogeneous void swelling near grain boundaries, is incomplete. In fact, by using a model formally very similar to the rate theory it is possible to describe experimental observations reasonably well. It is interesting that our conclusion agrees fully with the original formulation of the production bias model (PBM) by Woo and Singh^{45,46} who highlighted the significance of segregated coalescence of defects in collision cascades. Both the fact that in our model we use high values of the dislocation bias factor Z_i and that the expression for the rate of nucleation [Eq. (5)] was derived³⁸ using the PBM shows that our results fit squarely into the PBM framework. The fact that here the concept of one-dimensional diffusion of clusters was not used does not come as a surprise since the concept of PBM refers equally to pure materials and alloys, where in the first case the one-dimensional transport of interstitial clusters probably dominates the microstructural evolution while in the latter case the occurrence of long-range one-dimensional transport of interstitial defects is unlikely.

Finally, we would like to note the phenomenological aspect of the study described in this paper. The model proves to be capable of describing the experimentally observed phenomenon of heterogeneous void swelling in a somewhat better and more comprehensive way than other models currently available in the literature. The model shows that the origin of spatially heterogeneous void swelling may be associated with the heterogeneity in the distribution of dislocations near a grain boundary. This shows that the spatial distribution of the dislocation component of microstructure probably plays a determining part in the formation of the distribution of voids. Without a proper investigation of the evolution of the dislocation network it is difficult to draw conclusions about the actual cause of the large-scale spatial inhomogeneity of the void swelling profile in the vicinity of a grain boundary.

ACKNOWLEDGMENTS

This work was performed as a part of a collaborative program on modeling fusion materials sponsored by the International Energy Agency (IEA). We are grateful to R. Bullough, M. Victoria, G. Martin, and F. R. N. Nabarro for discussions and valuable advice, and we thank I. Cook and J. W. Connor for their encouragement and comments. We thank S. Golubov for the discussion that initiated this work, and we are grateful to B. N. Singh and H. Trinkaus for their

interest and criticism. Work at the Hong-Kong Polytechnic University was supported by University Grant Nos. G-T007 and G-T238, and also by grants PolyU 5167/01E and PolyU 5173/01E awarded by the Hong-Kong Research Grant Council. Work at the UKAEA Culham Science Center was funded by the UK Office of Science and Technology and by EURATOM.

APPENDIX A

In this appendix we describe a numerical approach to solving equations (3) and (4). We assume that we need to find these solutions on an interval $[0, L]$, where L is sufficiently large, so that $L\Omega_\infty \gg 1$. We split the entire interval of integration into $N \gg 1$ slices of equal length $l = L/N$. Within each slice function $\Omega^2(x)$ can be approximated by its value corresponding to the middle of the slice, so that for $x_i < x_{i+1}$ we have

$$\frac{d^2}{dx^2}\Pi(x) - \Omega_i^2\Pi(x) = 0, \quad (\text{A1})$$

where $\Omega_i^2 = \Omega^2([x_i + x_{i+1}]/2)$ and $x_N = L$. Function $\Omega^2(x)$ is now approximated by a discontinuous set of steplike segments. The solution of Eq. (A1) is a function that is continuous and differentiable everywhere on the interval $[0, L]$. Values of the derivative $d\Pi/dx$ and the solution $\Pi(x)$ at both sides of every slice $[x_i, x_{i+1}]$ are related via

$$\left. \frac{d\Pi(x)}{dx} \right|_{x_i} = \cosh(\Omega_i l) \left. \frac{d\Pi(x)}{dx} \right|_{x_{i+1}} + \Omega_i \sinh(\Omega_i l) \Pi(x_{i+1}),$$

$$\Pi(x_i) = \frac{\sinh(\Omega_i l)}{\Omega_i} \left. \frac{d\Pi}{dx} \right|_{x_{i+1}} + \cosh(\Omega_i l) \Pi(x_{i+1}). \quad (\text{A2})$$

Introducing the R -matrix by the relation $R_i = d \ln[\Pi(x)]/dx|_{x_i}$ and using Eqs. (A2), we find

$$R_{i+1} = \frac{\cosh(\Omega_i l) R_i + \Omega_i \sinh(\Omega_i l)}{\cosh(\Omega_i l) + \Omega_i^{-1} \sinh(\Omega_i l) R_i}, \quad (\text{A3})$$

or, conversely,

$$R_i = \frac{\cosh(\Omega_i l) R_{i+1} - \Omega_i \sinh(\Omega_i l)}{\cosh(\Omega_i l) - \Omega_i^{-1} \sinh(\Omega_i l) R_{i+1}}. \quad (\text{A4})$$

In the limit $x \rightarrow \infty$ we retain only the solution that falls off exponentially as a function of coordinate x . This corresponds to the boundary condition

$$R_N = -\Omega_\infty. \quad (\text{A5})$$

Using this boundary condition and Eq. (A4), we find values $R_{N-1}, R_{N-2}, \dots, R_0$. Solution $\Pi_+(x)$ that remains regular in the limit $x \rightarrow \infty$ can now be found recursively as

$$\Pi_+(x_{i+1}) = [\cosh(\Omega_i l) - \Omega_i^{-1} \sinh(\Omega_i l) R_{i+1}]^{-1} \Pi_+(x_i). \quad (\text{A6})$$

Boundary condition for $\Pi_+(x)$ at $x=0$ is $\Pi_+(0) = 1$.

Finding solution $\Pi_-(x)$ is somewhat more difficult. We choose the boundary condition on the *derivative* of $\Pi_-(x)$ at $x=0$ in the form $d \ln[\Pi_-(x)]/dx|_{x=0} = -R_0$, where R_0 equals the boundary value of the R -matrix found previously from Eqs. (A4) and (A5). We now impose the requirement following from Eq. (4) that the Wronskian of solutions $\Pi_-(x)$ and $\Pi_+(x)$ must be equal to $-K$. We write

$$\Pi_-(0) \left. \frac{d\Pi_+(x)}{dx} \right|_{x=0} - \Pi_+(0) \left. \frac{d\Pi_-(x)}{dx} \right|_{x=0} = -K. \quad (\text{A7})$$

Taking into account that $\Pi_+(0) = 1$, from (A7) we find the boundary condition on $\Pi_-(x)$

$$\Pi_-(0) = K [d \ln[\Pi_-(x)]/dx|_{x=0} - d \ln[\Pi_+(x)]/dx|_{x=0}]^{-1}. \quad (\text{A8})$$

Now values $\Pi_-(x_1), \Pi_-(x_2), \dots, \Pi_-(x_N)$ can be found using Eq. (A6). Finally, we write solution (4) in the form

$$\bar{\Pi}(x) = -\frac{\Pi_-(0)}{\Pi_+(0)} \Pi_+(x) \int_0^\infty \Pi_+(x') dx' + \Pi_+(x) \Pi_-(x) \times \left(\int_0^x \frac{\Pi_-(x')}{\Pi_-(x)} dx' + \int_x^\infty \frac{\Pi_+(x')}{\Pi_+(x)} dx' \right), \quad (\text{A9})$$

that contains no exponentially divergent terms and provides a convenient numerical representation of function $\bar{\Pi}(x)$.

APPENDIX B

In the case of a steplike distribution of the density of dislocations equation (3) has the form

$$\frac{d^2}{dx^2}\Pi(x) + K - \rho Z \Pi(x) \Theta(x - x_0) = 0. \quad (\text{B1})$$

In the interval $0 < x < x_0$ this equation has solution $\Pi(x) = -Kx^2/2 + Ax + B$. For $x > x_0$ the solution is $\Pi(x) = (K/Z\rho) + C \exp(-\sqrt{\rho Z}x)$. Using the boundary condition $\Pi(0) = 0$ we find that $B = 0$. Conditions of continuity of the solution and its first derivative at $x = x_0$ give rise to two more equations, using which it is possible to find constants A and C . By carrying out calculations, we arrive at

$$\Pi(x) = -\frac{Kx^2}{2} + \frac{x}{x_0} \left[\left(\frac{Kx_0^2}{2} + \frac{K}{\rho Z} \right) + \left(\frac{Kx_0^2}{2} - \frac{K}{\rho Z} \right) (1 + x_0 \sqrt{\rho Z})^{-1} \right] \quad (\text{B2})$$

for $0 < x < x_0$, and

$$\Pi(x) = \frac{K}{\rho Z} + \left(\frac{Kx_0^2}{2} - \frac{K}{\rho Z} \right) (1 + x_0 \sqrt{\rho Z})^{-1} \times \exp[-\sqrt{\rho Z}(x - x_0)], \quad (\text{B3})$$

for $x > x_0$. In the case shown in Fig. 1 this solution is indistinguishable from the solution found using the numerical algorithm described in Appendix A.

- ¹G. Martin, *Curr. Opin. Solid State Mater. Sci.* **3**, 552 (1998).
- ²K. Ehrlich, *Philos. Trans. R. Soc. London, Ser. A* **357**, 595 (1999).
- ³G. R. Odette, B. D. Wirth, D. J. Bacon, and N. M. Ghoniem, *MRS Bull.* **26**, 176 (2001).
- ⁴M. Samaras, P. M. Derlet, H. Van Swygenhoven, and M. Victoria, *Phys. Rev. Lett.* **88**, 125505 (2002).
- ⁵C. W. Chen and R. W. Buttry, *Radiat. Eff.* **56**, 219 (1981).
- ⁶B. N. Singh, T. Leffers, W. V. Green, and S. L. Green, *J. Nucl. Mater.* **105**, 1 (1982).
- ⁷M. Griffiths, R. W. Gilbert, and C. E. Coleman, *J. Nucl. Mater.* **159**, 405 (1988).
- ⁸S. J. Zinkle and B. N. Singh, *J. Nucl. Mater.* **283-287**, 306 (2000).
- ⁹A. J. E. Foreman, B. N. Singh, and A. Horsewell, *Mater. Sci. Forum* **15-18**, 895 (1987).
- ¹⁰A. D. Brailsford and R. Bullough, *J. Nucl. Mater.* **44**, 121 (1972); *Philos. Trans. R. Soc. London, Ser. A* **302**, 87 (1981).
- ¹¹H. Trinkaus, B. N. Singh, and A. J. E. Foreman, *J. Nucl. Mater.* **206**, 200 (1993).
- ¹²S. I. Golubov, B. N. Singh, and H. Trinkaus, *J. Nucl. Mater.* **276**, 78 (2000).
- ¹³S. L. Dudarev, *Phys. Rev. B* **62**, 9325 (2000).
- ¹⁴D. J. Bacon, A. F. Calder, and F. Gao, *J. Nucl. Mater.* **251**, 1 (1997).
- ¹⁵B. D. Wirth, G. R. Odette, D. Maroudas, and G. E. Lucas, *J. Nucl. Mater.* **244**, 185 (1997).
- ¹⁶B. D. Wirth, G. R. Odette, D. Maroudas, and G. E. Lucas, *J. Nucl. Mater.* **276**, 33 (2000).
- ¹⁷Yu. N. Osetsky, D. J. Bacon, A. Serra, B. N. Singh, and S. I. Golubov, *J. Nucl. Mater.* **276**, 65 (2000).
- ¹⁸S. L. Dudarev, *Phys. Rev. B* **65**, 224105 (2002).
- ¹⁹V. A. Borodin and A. I. Ryazanov, *J. Nucl. Mater.* **256**, 47 (1998).
- ²⁰B. N. Singh, *Radiat. Eff. Defects Solids* **148**, 383 (1999).
- ²¹S. L. Dudarev, in *Microstructural Processes in Irradiated Materials - 2000*, edited by G. E. Lucas, L. L. Snead, M. A. Kirk, and R. G. Elliman, MRS Symposia Proceedings No. 650 (Materials Research Society, Warrendale, PA, 2000), pp. R1.4.1–R1.4.6.
- ²²G. Martin (private communication). Molecular dynamics simulations of diffusion of interstitial clusters in an alloy performed by N.-V. Doan *et al.* (2002) showed that a moving cluster was confined between two solute atoms. The cluster escaped *via* a thermally activated process resulting in the change of the direction of its Burgers vector. Some aspects of this work were previously reported in N.-V. Doan, D. Rodney, and G. Martin, *Defect Diffus. Forum* **194-199**, 43 (2001).
- ²³T. S. Hudson, S. L. Dudarev, M. J. Caturla, and A. P. Sutton, Proceedings of the 132nd TMS Meeting, San Diego, CA, March 2003.
- ²⁴J. Marian, B. D. Wirth, J. M. Perlado, G. R. Odette, and T. Diaz de la Rubia, *Phys. Rev. B* **64**, 094303 (2001).
- ²⁵J. Marian, B. D. Wirth, A. Caro, B. Sadigh, G. R. Odette, J. M. Perlado, and T. Diaz de la Rubia, *Phys. Rev. B* **65**, 144102 (2002).
- ²⁶R. E. Stoller and G. R. Odette, *J. Nucl. Mater.* **141**, 647 (1986).
- ²⁷L. K. Mansur, in *Kinetics of Inhomogeneous Processes*, edited by G. R. Freeman (Wiley, New York, 1987), Chap. 8.
- ²⁸D. J. Bacon, D. M. Barnett, and R. O. Scattergood, *Prog. Mater. Sci.* **23**, 51 (1979).
- ²⁹F. R. N. Nabarro (private communication).
- ³⁰H. Van Swygenhoven, P. M. Derlet, and A. Hasnaoui, *Phys. Rev. B* **66**, 024101 (2002).
- ³¹P. M. Derlet and H. Van Swygenhoven, *Scr. Mater.* **47**, 719 (2002).
- ³²T. Diaz de la Rubia, H. Zbib, T. A. Khraishi, B. D. Wirth, M. Victoria, and M. J. Caturla, *Nature (London)* **406**, 871 (2000).
- ³³A. A. Semenov and C. H. Woo, *Appl. Phys. A: Mater. Sci. Process.* **73**, 371 (2001).
- ³⁴A. A. Semenov and C. H. Woo, *Appl. Phys. A: Mater. Sci. Process.* **74**, 639 (2002).
- ³⁵Grain boundary migration was recently observed in molecular dynamics simulations performed by M. Samaras, P. M. Derlet, H. Van Swygenhoven, and M. Victoria (private communication).
- ³⁶S. L. Dudarev, *Micron* **28**, 139 (1997).
- ³⁷A. A. Semenov and C. H. Woo, *Appl. Phys. A: Mater. Sci. Process.* **69**, 445 (1999).
- ³⁸A. A. Semenov and C. H. Woo, *Phys. Rev. B* **66**, 024118 (2002).
- ³⁹D. I. Norris, *J. Nucl. Mater.* **40**, 66 (1971).
- ⁴⁰B. N. Singh, M. Eldrup, S. J. Zinkle, and S. I. Golubov, *Philos. Mag.* **82**, 1137 (2002).
- ⁴¹F. Paschoud, Ph.D. thesis No. 834, Ecole Polytechnique Federale de Lausanne, 1990.
- ⁴²C. B. A. Forty, R. A. Forrest, D. J. Compton, and C. Rayner, *Handbook of Fusion Activation Data. Part 1: Elements Hydrogen to Zirconium*, UKAEA Fusion Report 180 (1992), *Part 2: Elements Niobium to Bismuth*, UKAEA Fusion Report 232 (1993).
- ⁴³D. Rodney and G. Martin, *Phys. Rev. B* **61**, 8714 (2000).
- ⁴⁴H. M. Huang and N. M. Ghoniem, *Comput. Mater. Sci.* **23**, 225 (2002).
- ⁴⁵C. H. Woo and B. N. Singh, *Philos. Mag.* **65**, 889 (1992).
- ⁴⁶B. N. Singh and A. J. E. Foreman, *Philos. Mag.* **66**, 975 (1992).